



Research article

An analysis of the vaginal microbiota and cervicovaginal metabolomics in cervical lesions and cervical carcinoma

Jie Ou, Yanan Kang, Medlegeh, Kun Fu, Yu Zhang^{*}, Wenqing Yang^{**}

Department of Gynecology, Xiangya Hospital Central South University, Changsha, Hunan, 410008, China

ARTICLE INFO

Keywords:

Cervical intraepithelial neoplasia
Cervical carcinoma
Metabolome
Microbiota
Genital inflammation

ABSTRACT

Background: To explore the role of vaginal microbiota and metabolomics in the progression of cervical dysplasia.

Methods: The patient group consists of female patients with low-grade, high-grade cervical dysplasia, and cervical cancer. Normal cervix samples from health volunteers were used as controls. The metabolic fingerprints of cervicovaginal lavage were analyzed using liquid chromatography-mass spectrometry, while the vaginal microbiota was examined through 16S rRNA sequencing. Bioinformatic analysis was adopted to investigate the interplay between hosts and microbes. The vaginal metabolic and microbiota profiles of 90 female patients with cervical dysplasia and 10 controls were analyzed to discover the biological characteristics underlying the progression of cervical cancer.

Results: We found that Valyl-Glutamate, N, N'-Diacetylbenzidine, and Oxidized glutathione, which were involved in oxidative stress response, were discriminators to distinguish the normal cervix, invasive cervical carcinomas, and CIN3 from others. Cervical carcinoma was characterized by a large variety of vaginal microbes (dominated by non-Lactobacillus communities) compared to the control. These microbes affected amino acid and nucleotide metabolism, producing metabolites with cervical carcinoma and genital inflammation compared to the control group.

Conclusions: This study revealed that cervicovaginal metabolic profiles were determined by cervical cancer, vaginal microbiota, and their interplays. ROS metabolism can be used to discriminate normal cervix, CIN3, and invasive cervical carcinoma.

1. Introduction

Cervical carcinoma is the fourth most diagnosed cancer globally in women [1]. Although HPV infection is the main cause of cervical carcinogenesis, over 90 % of HPV infections are transient and cleared by immune responses. Merely 0.6–3% of patients with persistent HPV infection develop carcinoma [2], indicating that persistent infection is essential for the development of high-grade CIN and

Abbreviations: AUC, Area Under the Curve; CVL, cervicovaginal lavage; HMDB, Human Metabolome Database; HPV, high-risk papillomavirus; LD, Lactobacillus-dominant; NLD, non-Lactobacillus-dominant; OPLS-DA, Orthogonal Partial Least-Squares-Discriminant Analysis; PCoA, principal co-ordinate analysis; PLS-DA, Partial Least-Squares-Discriminant Analysis; ROC, Receiver Operating Characteristics; VIP, Variable Importance of Projection.

* Corresponding author.

** Corresponding author.

E-mail addresses: xyzhangyu@csu.edu.cn (Y. Zhang), xywenqingyang@csu.edu.cn (W. Yang).

<https://doi.org/10.1016/j.heliyon.2024.e33383>

Received 14 December 2023; Received in revised form 16 May 2024; Accepted 20 June 2024

Available online 22 June 2024

2405-8440/© 2024 The Authors. Published by Elsevier Ltd. This is an open access article under the CC BY-NC license (<http://creativecommons.org/licenses/by-nc/4.0/>).

cervical cancer. Consistently, cervicovaginal microbiota reportedly play a substantial role in the persistence or regression of virus infection and disease progression [3].

Vaginal microbiota forms a layer of protection to reduce pathogen infection, thereby maintaining the hemostasis of the cervicovaginal microenvironment [4]. Consequently, microbial dysbiosis significantly contributes to the progression of cervical neoplasia and cervical carcinogenesis [5]. Epidemiological studies have revealed that the diversity of the non-*Lactobacillus*-dominated vaginal microbiome is closely associated with HPV infection [6–10]. A meta-analysis of cross-sectional and longitudinal studies also revealed that women with a non-*Lactobacillus*-dominant vaginal microbiome or a *L. iners*-dominant vaginal microbiome had 2–3 times higher odds of high-risk HPV prevalence and cervical neoplasia, as well as 3–5 times higher odds of prevalent HPV (95 % CI) than women with a *L. crispatus*-dominant vaginal microbiome [11].

Microbial metabolites in the vaginal microenvironment, such as lactic acid, exert antitumor effects. For example, the *L. crispatus*-dominated microbiota produces high levels of D-lactate, which inhibits carcinoma cell growth [12]. Moreover, vaginal lactobacilli exhibit cytotoxic effects on cervical tumor cells independent of pH and lactic acid in vitro [13]. Therefore, increasing attention has been paid to the metabolites in the microenvironment [14]. Combined with advances in metabolomics, it is well accepted that the metabolites of vaginal microbiota form a bridge between microbes and the host [15]. Metabolites, such as H₂O₂ and bacteriocin, have been implicated in CIN and carcinogenesis. However, comprehensive profiling studies of the microbial metabolism in the cervicovaginal microenvironment are still lacking. Here, we aim to elucidate the metabolomic profiles of cervicovaginal lavage and vaginal microbiota in normal, low- and high-grade CIN and carcinoma patients. Finally, bioinformatic analysis was applied to investigate the interaction between vaginal microbes and their hosts.

2. Materials and methods

2.1. Patients

According to the histological examination of colposcopy-directed biopsy samples or cervical conization tissues, 100 non-pregnant female patients out of 200 patients diagnosed at Central Southern University Xiangya Hospital from January to October 2021 were recruited. Patients with following situations were excluded from the study: active menstruation; recent use (within the previous month) of antibiotics (n = 20), antifungals or antivirals (n = 3); current or recent (within the previous 2 weeks) vaginal infection (including bacterial vaginosis) (n = 23), vulvar infection, urinary tract, or sexually transmitted infections (such as chlamydia, gonorrhea, trichomoniasis, or genital herpes) (n = 11); HIV-positive (n = 2); recent use (within 48 h before the visit) of douching substances, vaginally applied medications, feminine deodorant sprays, or vaginal lubricants (n = 9); sexual intercourse (less than 48 h before the visit) (n = 5); a diagnosis of type I or II diabetes (n = 16); body mass index (BMI) ≥ 30 (n = 11). The participants were grouped as follows: cervix without neoplasia (N group, n = 10), cervical intraepithelial neoplasia I (CIN 1 group, n = 15), CIN 2 (n = 25) group, CIN 3 (n = 25) group, and invasive cervical carcinoma (ICC, n = 25) group.

All of the details were obtained and verified via pelvic examination by an experienced physician, medical records questionnaires, and follow-up by telephone calls. The study was approved by the ethics committee of Xiangya Hospital of Central South University (Approval No.: 202101030), and written informed consent from each participant was obtained.

2.2. Sample collection

Vaginal swabs and cervicovaginal lavage (CVL) samples were collected during the first visit before any operations including colposcopy examination and conization by an experienced gynecological clinician. The clinician inserted a speculum without the use of lubricant and obtained a vaginal swab by swabbing the lateral walls of the upper vaginal cavity in the direction of 5–6 o'clock. The swab was promptly stored in a sterile Eppendorf tube. Subsequently, 10 mL of sterile 0.9 % saline solution was used to collect CVL samples. Both the vaginal swab and CVL samples were immediately placed on ice and were then frozen at -80°C within 30 min. CVLs were thawed on ice and subsequently centrifuged at $700\times g$ for 10 min at 4°C . DNA was extracted from vaginal swabs using the PowerSoil DNA Isolation Kit (MO BIO Laboratories, Carlsbad, CA, USA) following the manufacturer's instructions. CVL samples and extracted DNA were aliquoted and stored at -80°C for further analysis.

2.3. Vaginal microbiota

DNA from vaginal swabs was extracted as described before [6]. PCR amplification from genomic DNA was performed using barcode primers and TksGflex DNA polymerase (Takara). The V3–V4 (or V4–V5) variable regions of 16S rRNA genes were amplified by universal primers, 343 F and 798 R (or 515F and 907R for V4–V5 regions) to analyze bacterial diversity [16]. Library sequencing and data processing were performed with OE Biotech Co., Ltd. (Shanghai, China).

The Shannon–Weaver index was calculated at both the species and genus levels to assess bacterial diversity using the R package vegan [17]. Furthermore, the Bray–Curtis dissimilarity indices were computed at the species level using the R and package vegan, following the square root transformation and Wisconsin double standardization of reads [17]. To assess the between-sample (β) diversity, multivariate analysis of variance (MANOVA) was conducted using the Bray–Curtis distances [17]. Additionally, principal co-ordinate analysis (PCoA) was executed based on the Bray–Curtis dissimilarity matrix to visualize β diversity [17]. The present study employed Orthogonal Partial Least-Squares-Discriminant Analysis (OPLS-DA) and Partial Least-Squares-Discriminant Analysis (PLS-DA) to differentiate the metabolites that exhibit inter-group variations [16]. To mitigate the risk of overfitting, the model's

reliability was assessed using 7-fold cross-validation and 200 Response Permutation Testing (RPT) iterations [16]. The Variable Importance of Projection (VIP) scores derived from the OPLS-DA model were used to rank the relative contribution of each variable toward group discrimination [16]. The statistical significance of differential metabolites between groups was assessed using a Two-tailed Student's t-test. Differential metabolites were selected based on VIP values greater than 1.0 and p-values less than 0.05.

2.4. Cervicovaginal metabolomics

The ACQUITY UPLC I-Class ultra-performance liquid chromatography in tandem with IMS Q-TOF high-resolution mass spectrometry (LC-MS) was used for the analysis. The extract was gradually eluted from a C18 column (Waters UPLC BEH C18–2.1 × 100 mm, 1.7 μm) using water and methanol containing 0.1 % formic acid (FA). The analytical method was optimized based on compound polarity or hydrophilicity [12]. The MS analysis was performed under positive and negative ion scanning modes, with a scan range of 50–1000 amu. The variability of extraction and instrumentation was validated based on the recovery and internal standards [18]. A technical replicate was created by pooling a composite sample comprising a small volume of each experimental sample with extracted water samples as blanks [18]. To monitor instrument stability, these control samples were evenly distributed among the injections.

The LC-MS data were analyzed using Progenesis QI V2.3 (Nonlinear, Dynamics, Newcastle, UK) for baseline filtering, peak identification, integral, retention time correction, peak alignment, and normalization [12]. The primary parameters utilized were 5 ppm precursor tolerance, 10 ppm product tolerance, and 5 % product ion threshold [12]. Compounds were identified by screening various databases, including the Human Metabolome Database (HMDB), Lipidmaps (V2.3), METLIN, EMDB, PMDB, and self-built database with the precise mass-to-charge ratio (M/z), secondary fragments, and isotopic distribution [16]. After extraction, the data were processed by peak elimination with a missing value (ion intensity = 0) in over 50 % of groups, zero substitution with half of the minimum value, and screening based on the qualitative results of the compound [16]. Compounds with the scores below 36 (out of 60) were considered imprecise and were subsequently eliminated. The data matrix consisted of positive and negative ion data [16].

K-means clustering was adopted to assess the overall change trend of metabolites between groups. Using the geometric space generated by metabolite matrices that exhibited significant differences between groups, patients were categorized into clusters based on proximity criteria utilizing the k-means algorithm [12]. The algorithm comprises the following steps: 1) Placing K points into the space represented by the patients being clustered, which represent initial group centroids; 2) Assigning each patient to the group with the closest centroid; 3) Recalculating the positions of the K centroids once all patients have been assigned [12]. Repeat Steps 2 and 3 until the centroids reach immobility, thereby grouping patients into homogenous groups to maximize heterogeneity across the groups [12]. The optimal number of clusters is determined by the solution that yields the highest Calinski-Harabasz index value [18]. To evaluate the internal quality of the clusters, the stability of the optimal solution was assessed by computing Jaccard bootstrap values through 100 iterations [18]. A high degree of stability is indicated by average Jaccard similarities of 0.85 or greater [12].

2.5. Statistical analyses

The microbiota was categorized into Lactobacillus-dominant (LD) or non-Lactobacillus-dominant (NLD) based on a threshold of 80 % relative abundance of Lactobacillus [19]. The status of genital inflammation was presented by the infiltration of pro-inflammatory cells, which were divided into low and high infiltration groups based on the leucocyte number per high power field (HPF), where 5–25 cells/HPF was classified as low infiltration and over 25 cells/HPF as high. The data were logged for statistical analysis. Receiver Operating Characteristics (ROC) analysis was used to identify the metabolites that differentiated patients in the ICC group from those in the control group [18]. The discriminatory power of the metabolites was evaluated based on the Area Under the Curve (AUC) values, with AUC values greater than 0.8 as strong discriminators [18]. An analysis of variance (ANOVA) was employed to examine the demographic variables among patient groups, including age, vaginal pH levels, and metabolite concentrations. Fisher's exact test was used for categorical variables such as smokers' number and inflammation status. P-values <0.05 were considered statistically different. All the data was uploaded online for public access.

3. Results

3.1. Cervical cancer patients exhibited different metabolite profiles from control and CIN patients

We characterized the cervicovaginal metabolomes of non-pregnant individuals from normal cervix group (N group) (n = 10), women with cervical intraepithelial neoplasia 1 (CIN1 group) (n = 15), CIN2 group (n = 25), CIN3 group (n = 25), and newly diagnosed invasive cervical carcinoma (ICC group) (n = 25) using a global metabolomic approach. Participants were grouped based on the histology of colposcopy-directed biopsy samples or conization tissues, which were evaluated by two pathologists with specialized training. [Supplementary Table S1](#) provides a comprehensive overview of the patient's characteristics and demographic information. Differences in age, status of genital inflammation, and liquid-based cytology descriptions were found between the groups (p < 0.05).

A total of 1723 compounds were identified in our metabolome dataset, including 3 hydrocarbons, 7 alkaloids and derivatives, 47 phenylpropanoids and polyketides, 48 nucleosides, 61 aromatics, 110 heterocyclic compounds, 433 organic acids and derivatives, 576 lipids and lipid-like molecules, 435 xenobiotics, and 2 partially characterized molecules.

The Partial Least Squares-Discriminate Analysis (PLS-DA) of the cervicovaginal lavage (CVL) samples of various groups revealed that the global metabolomic profiles of ICC patients were distinct from those of other groups in principal component 1 (PC1) and PC2

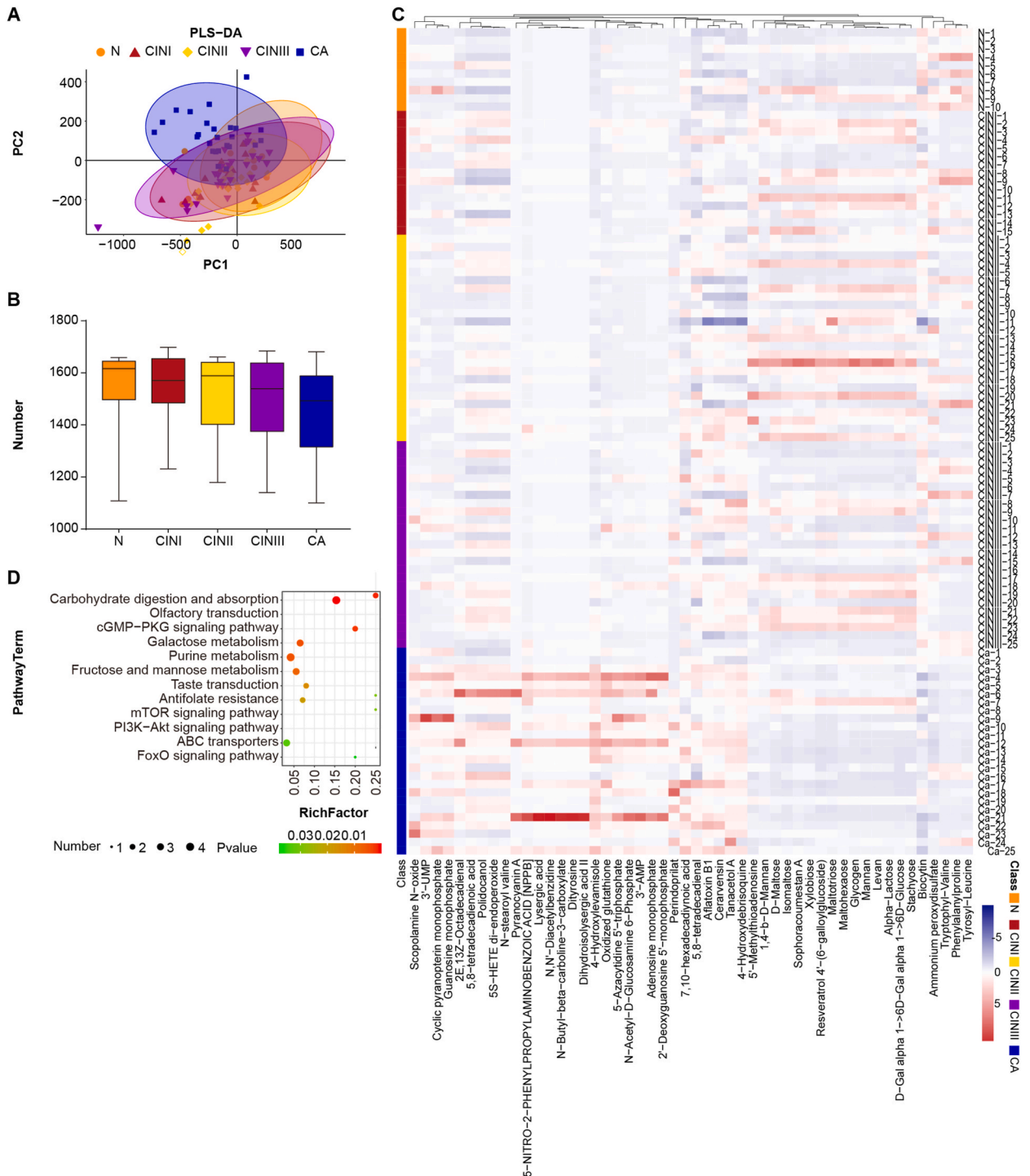


Fig. 1. Cervicovaginal metabolites are associated with cervical lesions. **A.** Partial least squares-discriminant analysis (PLS-DA) of cervicovaginal lavage (CVL) samples from different groups illustrated that global metabolomic profiles of ICC patients were distinct from other groups on principal component 1 (PC1) and PC2 (MANOVA, Wilk's lambda test, $p = 0.006$). **B.** 1465 \pm 155 metabolites in ICC patients, 1538 \pm 190 in the N group (Mann-Whitney U test, $p = 0.08$), 1554 \pm 133 in CIN 1 (Mann-Whitney U test, $p = 0.056$), 1515 \pm 144 in CIN 2 (Mann-Whitney U test, $p = 0.211$) and 1500 \pm 165 in CIN 3 (Mann-Whitney U test, $p = 0.308$), with no significant difference in the number of the metabolites between groups. **C.** Metabolomic heatmap showing that metabolites in cervical carcinoma form a unique cluster different from other groups. **D.** The unique metabolites in the ICC group were lipids and organic acids or were related to the carbohydrate digestion and absorption pathways.

(Fig. 1A; MANOVA, Wilk's Lambda test, $p = 0.006$). Furthermore, Fig. 1B indicates that the number of distinct metabolites in the N and CIN 1-CIN 3 groups was similar to that in the ICC group. There were 1465 ± 155 metabolites in ICC patients, 1538 ± 190 in the N group (Mann-Whitney U test, $p = 0.08$), 1554 ± 133 in CIN 1 (Mann-Whitney U test, $p = 0.056$), 1515 ± 144 in CIN 2 (Mann-Whitney U test, $p = 0.211$), and 1500 ± 165 in CIN 3 (Mann-Whitney U test, $p = 0.308$) groups (Fig. 1B).

Furthermore, we found that metabolite distribution was the primary source of differences in metabolic profiles. To assess metabolic profiles, we compared the shared and unique metabolites among groups. Our analysis revealed that 86% (1481/1723) of the identified metabolites were shared by all the groups. The ICC group exhibited the highest number of unique metabolites ($n = 11$), followed by 6 in the N group, 3 in the CIN 1 group, and one each for the CIN 2 and 3 groups (Supplementary Fig. S1). The unique metabolites for the ICC group were lipids and organic acids as revealed by a heatmap of the metabolites (Fig. 1C). These unique lipids and acids were mainly involved in carbohydrate digestion and absorption (Fig. 1D) (Supplementary Tables S2-S5).

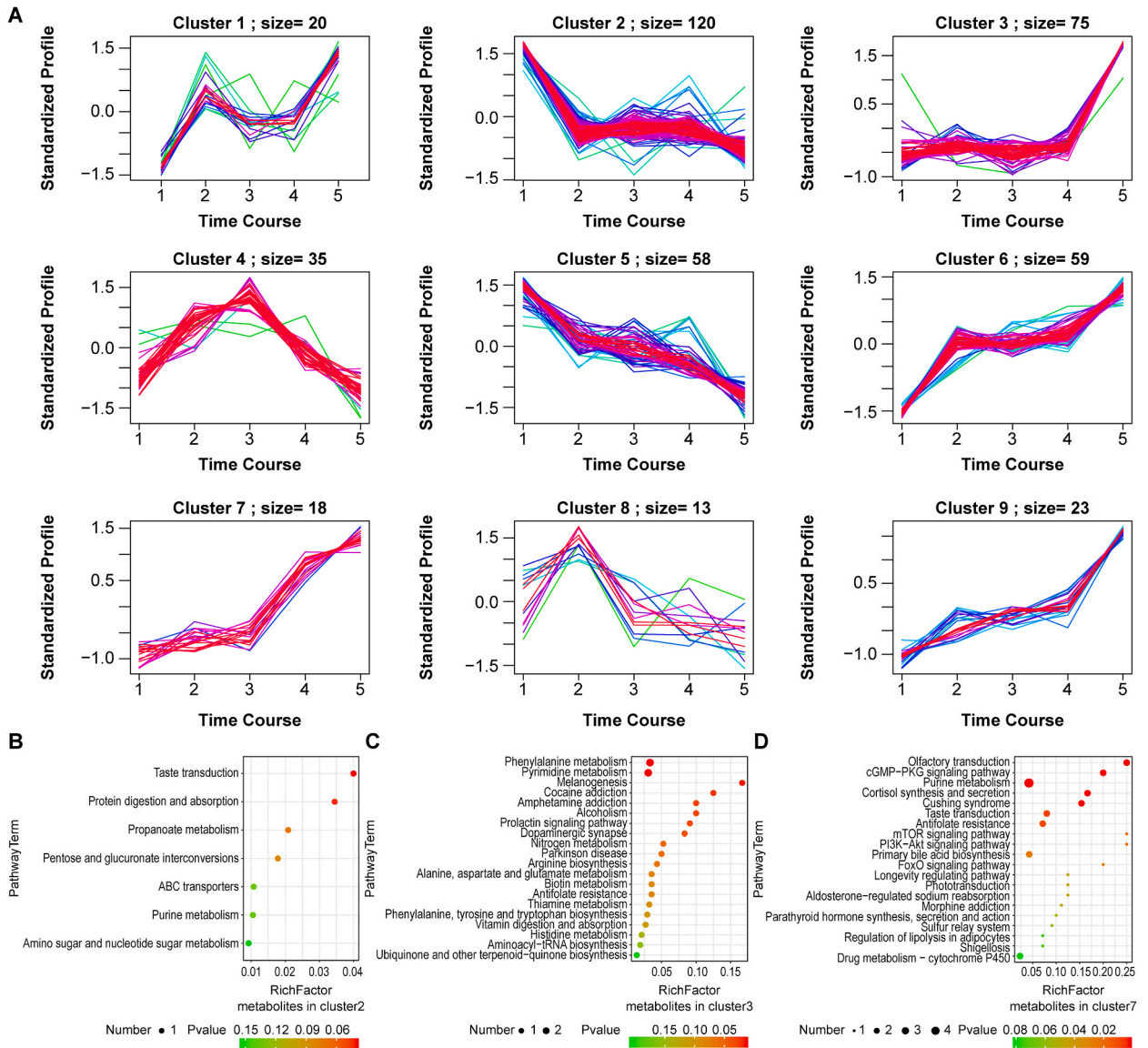


Fig. 2. Cervicovaginal metabolites trend from normal to CIN and then to ICC patients. A total of 421 metabolites were selected using the k-means clustering algorithm with significant differences among groups (ANOVA, $p < 0.05$), and divided into 9 clusters with different change trends among groups. B. Metabolites in cluster 2, showing a sharp decrease from N to CIN 1 and no change in further progression, included 120 metabolites mainly related to protein digestion and absorption or carbohydrate metabolism, including propanoate and pentose-glucuronate interconversions; C. Cluster 3, consisting of 75 metabolites from phenylalanine and pyrimidine metabolism pathways exhibited a definite increase in ICC compared to all the other groups; D. 18 metabolites showing higher concentrations in CIN3 group than the others in Cluster 7, mainly from the purine metabolism pathway.

3.2. Specific metabolites were identified as potential biomarkers of normal, CIN, and ICC

To explore the association between patients and cervicovaginal metabolome, we detected the trend of changes in distinctive metabolites across all the groups using the k-means clustering algorithm. A total of 421 metabolites with significant differences among groups (ANOVA, $p < 0.05$) were selected and divided into 9 clusters according to different change trends (Fig. 2A). Cluster 2 showed a sharp decrease from N to CIN 1, containing 120 metabolites that are related to protein digestion and absorption, as well as carbohydrate metabolism including propanoate and pentose-glucuronate interconversions (Fig. 2B). Cluster 3, consisting of 75 metabolites from phenylalanine and pyrimidine metabolism pathways, exhibited a definite increase in ICC (Fig. 2C). Moreover, 18 metabolites, which are mainly involved in the purine metabolism pathway, exhibited higher concentrations in the CIN3 group than in Cluster 7, (Fig. 2D). Distinctively, Cluster 5 containing 58 metabolites showed a continuous decreasing trend from the normal to CIN and ICC groups, indicating the possible changes in the metabolic spectrum of ICC (Fig. S)

Given the distinct metabolomes observed among the patient group, we proceeded to examine the respective signatures of these groups through the receiver operating characteristic (ROC) analysis. As illustrated in Fig. 3, the specific metabolite, Valyl-Glutamate, distinguished the normal samples from the others with an AUC value of 0.865 (Fig. 3E), which is lower in normal patients (Fig. 3A). Moreover, using ROC analysis, we identified N, N'-Diacetylbenzidine and oxidized glutathione as discriminators that distinguish ICCs, with AUC values of 0.847 and 0.842, respectively (Fig. 3F–G). Notably, the concentrations of these metabolites were significantly higher in the ICC group (Fig. 3B–C). 4-Hydroxydebrisoquine, whose concentrations were higher in the CIN3 group (Fig. 3D), was a discriminator that differentiates the CIN3 group from the others with a value of 0.827 (Fig. 3H).

3.3. Vaginal microbiota in cervical cancer patients differs from control and CIN patients

Following 16S RNA sequencing, a principal coordinate analysis (PCoA) with the Bray-Curtis dissimilarity index was conducted to identify significant differences in bacterial composition between carcinoma samples and controls (Fig. 4A) (permutational multivariate analysis of variance, MANOVA, $p = 0.001$). The presence of greater bacterial diversity in carcinoma patients was confirmed by a high Shannon-Wiener index at the species level compared to N, CIN 1, CIN 2, and CIN 3 (Fig. 4B) (pairwise Wilcoxon rank-sum test, p

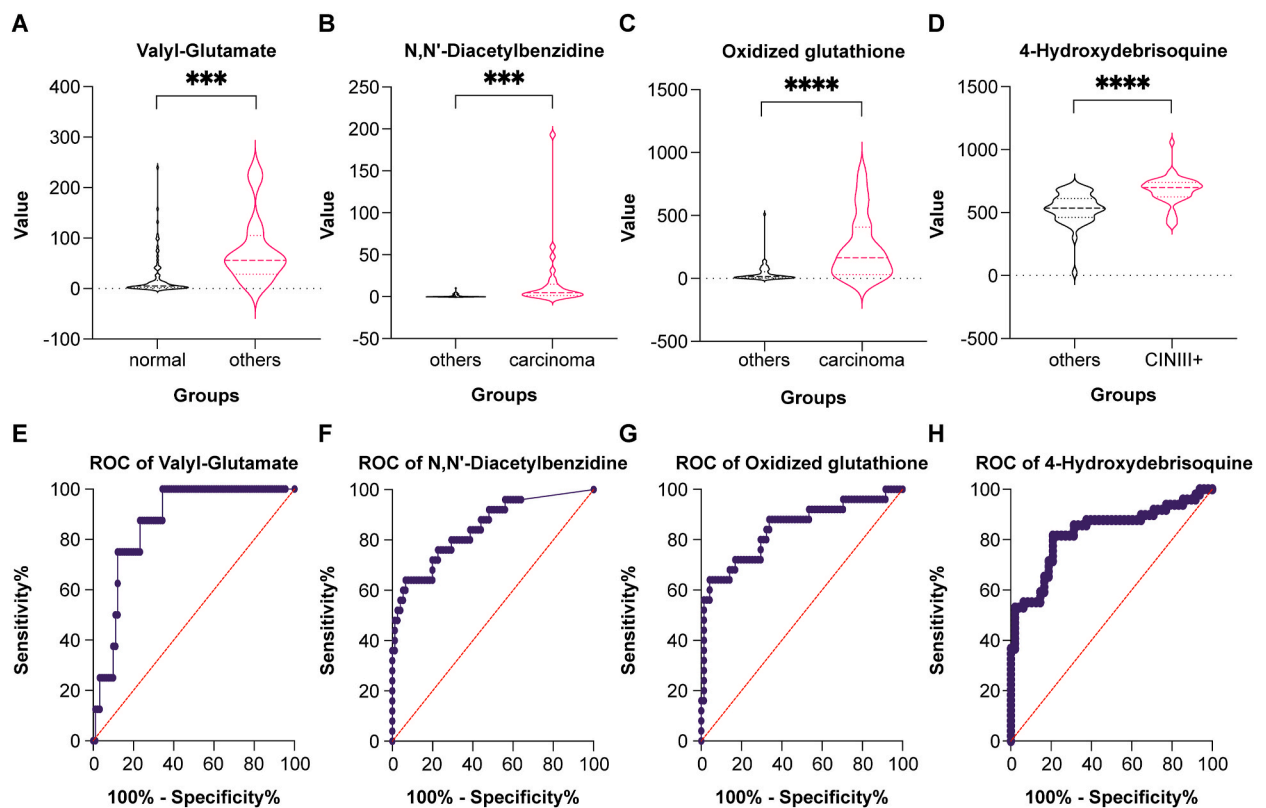


Fig. 3. Specific metabolites were identified as potential biomarkers of normal, CIN and ICC. A. concentration of Valyl-Glutamate in the normal and the others ($p = 0.0002$); B–C. concentrations of N,N'-Diacetylbenzidine and Oxidized glutathione in the ICCs and the others ($p1 < 0.0001$, $p2 < 0.0001$); D. concentration of 4-Hydroxydebrisoquine in the CIN3 patients and the others ($p < 0.0001$); E. ROC of Valyl-Glutamate in the normal and the others (AUC = 0.865, $p = 0.0006$); F–G. ROC of N,N'-Diacetylbenzidine and Oxidized glutathione in the ICCs and the others (AUC1 = 0.847, $p < 0.0001$, AUC2 = 0.842, $p < 0.0001$); H, ROC of 4-Hydroxydebrisoquine in the CIN3 patients and the others (AUC = 0.827, $p < 0.0001$).

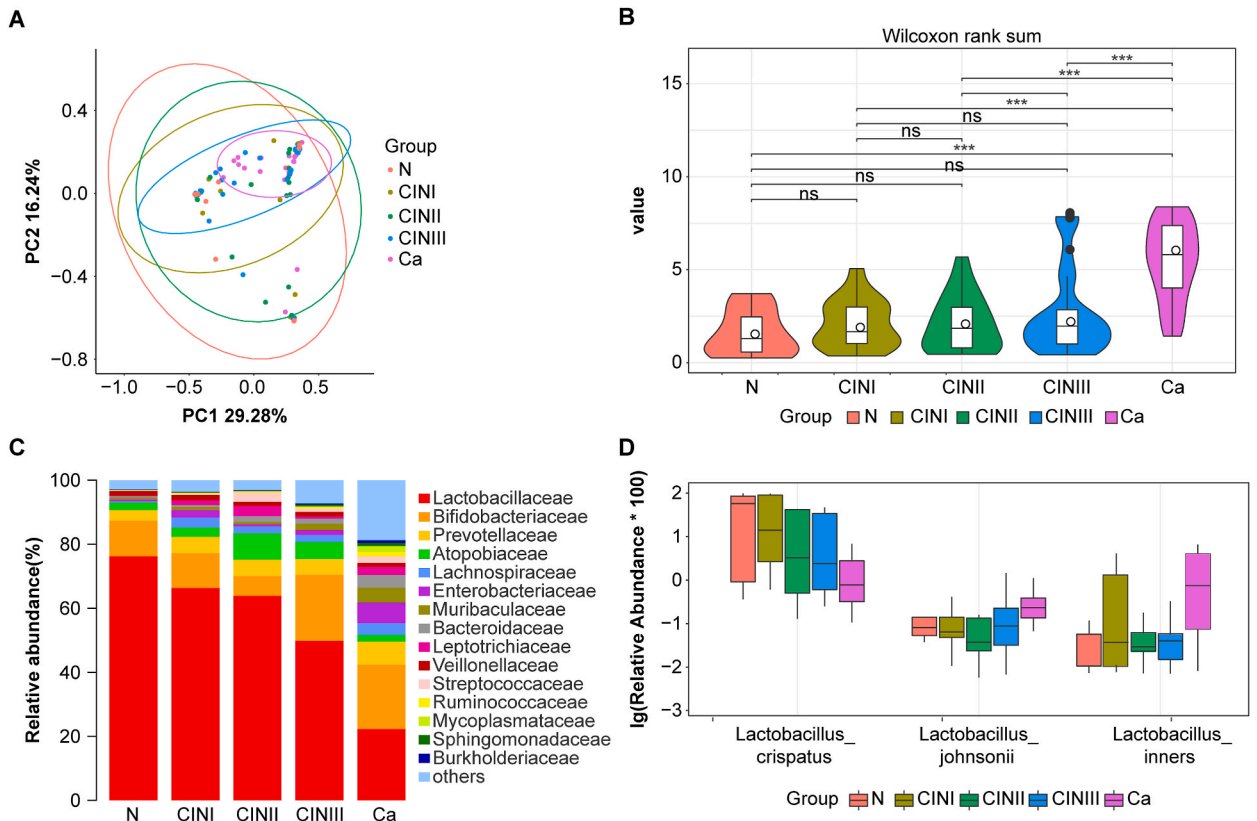


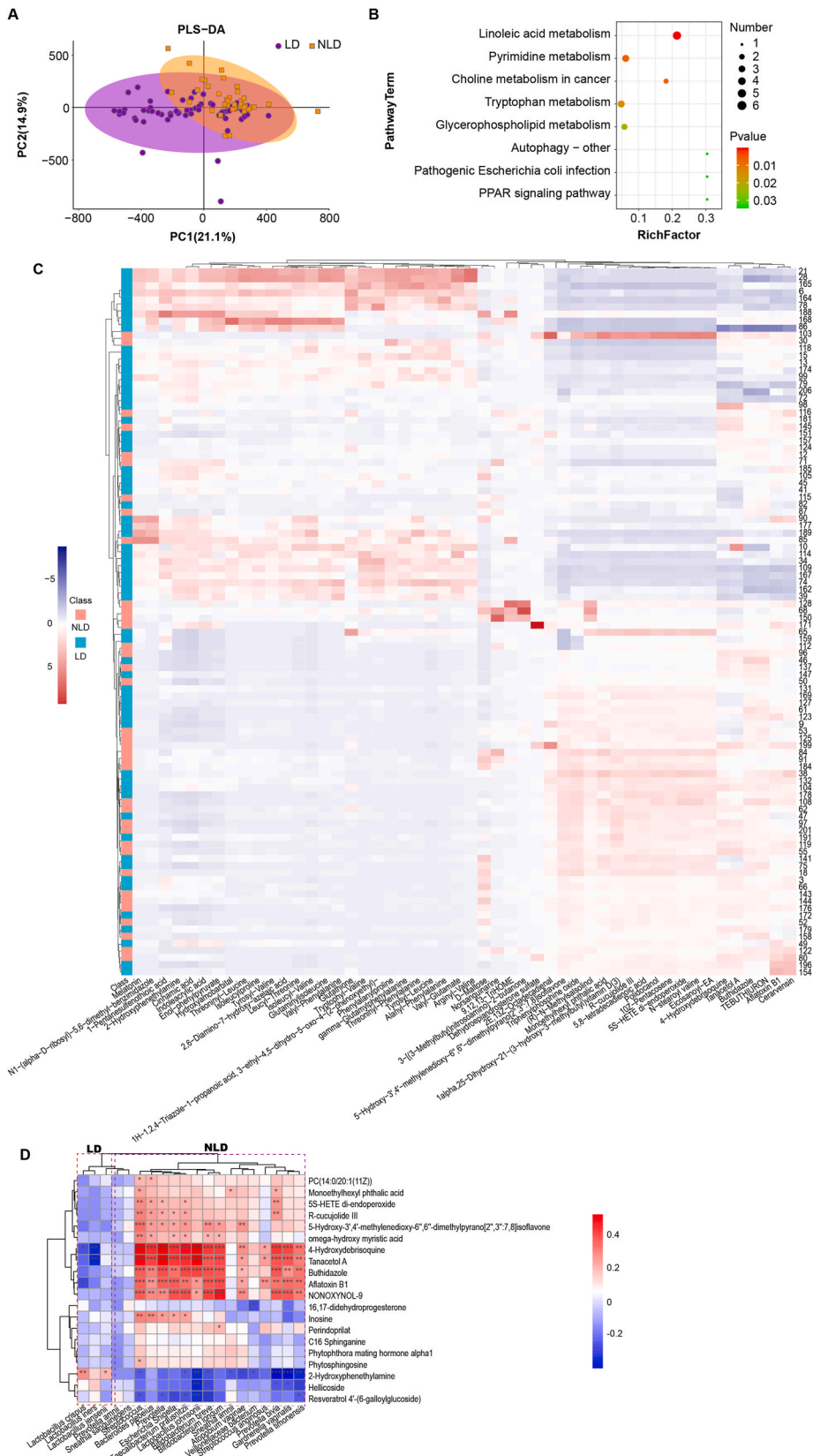
Fig. 4. Vaginal microbiota in cervical cancer patients differed from control and CIN patients. A. PCA based on the Bray-Curtis dissimilarity index of bacterial composition between carcinoma samples and controls in different groups, MANOVA, $p = 0.001$; B. Shannon-Wiener index of ICC at the species level compared to N, CIN 1, CIN 2 and CIN 3, respectively (pairwise Wilcoxon rank-sum test, $p < 0.001$); C. compared to the N group, the dominance of *Lactobacillus* communities decreased with the progression of cervical dysplasia, and the ICC group had the highest diversity of microbes, which was dominated by non-*Lactobacillus* taxa such as Prevotellaceae, Streptococcaceae, and Atopobiaceae; D. *Lactobacillus crispatus* was dominant in the N group and decreased in patient groups, with complete depletion in the ICC group. By contrast, the abundance of *L. johnsonii* and *L. iners* was higher in the ICC group (ANOVA, $p < 0.001$).

< 0.001). Similarly, high microbial diversity in patients with cervical carcinoma has been reported. We next identified different microbes in the patients at the genus and species level. Compared to the N group, the *Lactobacillus* community was dominated in the N group, however, its proportion was diminished with the progression of cervical dysplasia. The diversity of metabolites in the ICC group was the greatest, with non-*Lactobacillus* taxa such as Prevotellaceae, Streptococcaceae, and Atopobiaceae being the dominant ones (Fig. 4C). At the species level, *Lactobacillus crispatus* was dominant in the N group, but it was less abundant in the patient groups, with complete depletion in the ICC group. In contrast, the abundance of *L. johnsonii* and *L. iners* was higher in the ICC group (ANOVA, $p < 0.001$) (Fig. 4D).

3.4. Vaginal microbiota is associated with cervicovaginal metabolites

Cervicovaginal microbiota directly affects the cervicovaginal microenvironment through metabolite production that is crucial for cervicovaginal health. We investigated whether the discrepancies in vaginal microbiota accounts for the observed variations in the metabolome dataset. By the PLS-DA plots of the samples based on microbiota composition, we observed that the metabolomes of patients contained *Lactobacillus*-dominated (LD) vaginal microbiota, forming a distinct cluster from the non-*Lactobacillus*-dominated (NLD) microbiota (Fig. 5A). This difference was particularly pronounced on PC1, which accounted for 21.1 % of the variation in the dataset and was statistically significant according to the Mann-Whitney U test ($p = 0.002$). As shown in Fig. 5C, the metabolome dataset was clustered into two clusters by LD and NLD, and the metabolites enriched in NLD were also enriched in the ICC group. These metabolites were involved in linoleic acid metabolism and pyrimidine metabolism pathways (Fig. 5B), providing evidence of the regulation of the profiles of cervicovaginal metabolites by the cervicovaginal microbiome.

We then assessed the relationship between the 20 differential metabolites and the 20 validated differential species using Spearman's correlation. We found that the taxa enriched in carcinoma, such as *Streptococcus*, *Prevotella* and *Gardnerella*, were positively correlated with the metabolites enriched in carcinoma, such as aflatoxin B1 and 4-hydroxydebrisoquine but were negatively correlated with the metabolites enriched in controls, such as hellicoside and 2-hydroxyphenethylamine. These metabolites enriched in



(caption on next page)

Fig. 5. Vaginal microbiota influencing the cervicovaginal metabolome. A. PLS-DA plots based on microbiota composition and metabolomes for patients with *Lactobacillus*-dominated (LD) vaginal microbiota formed a cluster significantly different from the metabolomes from patients with non-*Lactobacillus* dominance (NLD) PC1 (Mann-Whitney *U* test, $p = 0.002$); B. Metabolomic heatmap showing two clusters according to LD and NLD; C. Metabolites enriched in NLD were also enriched in the ICC group, and were related to linoleic acid metabolism and pyrimidine metabolism pathways; D. Spearman's correlation between the 20 differential metabolites and the 20 validated differential species.

carcinoma reliably distinguished carcinoma from controls. Consistently, the species enriched in control samples were positively correlated with the metabolites from control samples, while negatively correlated with metabolites enriched in carcinoma. These results revealed a homogenous metabolic interplay between the vaginal microbiota and the host (Fig. 5D), providing the evidence for metabolites as the indicators of cervical carcinoma.

3.5. The inflammatory microenvironment is related to metabolites in the cervicovaginal microenvironment and vaginal microbiota

Given the pivotal role of inflammation in tumor progression, we further examined the potential correlation between the cervicovaginal metabolome and genital inflammation, which is primarily characterized by the infiltration of pro-inflammatory immune cells. As shown in Fig. 6A, the genital inflammation status, was significantly different between the high and low groups, according to the metabolome (MANOVA, Wilk's lambda test, $p = 0.001$) both on PC1 and PC2 (Mann-Whitney *U* test, $p = 0.002$). Based on the high and low status of genital inflammation, the metabolome revealed two clusters of patients (Fig. 6B), and the patients with high status of genital inflammation exhibited higher concentrations of metabolites related to the biosynthesis of unsaturated fatty acids (Fig. 6C).

Vaginal microbiota impacts cervical neoplasia and carcinoma via inflammation caused by non-*Lactobacillus* species. To better understand the relationship between microbiota and inflammation in cervical dysplasia progression, we analyzed the correlation between the high status of genital inflammation and LD microbiota and between the low status of inflammation and NLD microbiota. The results indicated that oxidized glutathione was positively correlated with adenosine monophosphate, N-acetyl-D-glucosamine 6-phosphate, and 3'-AMP, all drastically elevated in the ICC group (Fig. 6D).

4. Discussion

Metabolic profiling of cervicovaginal lavages provides great insight into the interplay between the host and vaginal microbiota. Four detected metabolites, namely, oxidized glutathione, aflatoxin B1, 4-hydroxydebrisoquinie, and trimeprazine, can reliably distinguish ICC patients from healthy individuals. The reduction in the abundance of vaginal *Lactobacillus* species is associated with the microenvironment where immunosuppressors and oxidation products accumulate. Our study also revealed that the metabolic profiles of CVL samples are influenced by vaginal microbiota and genital inflammation and represent fundamental differences between normal cervix and cervical carcinoma, deepening the understanding of the interplay of microbes and hosts in cervical carcinogenesis and providing predictors of patients' status.

Vaginal microbiota is known to be closely related to genital inflammation [20] and cervical carcinogenesis [21]. A decrease in the abundance of vaginal *Lactobacillus* species was associated with the risk of cervical neoplasia and cervical cancer. However, the underlying biological and molecular mechanisms remain understudied.

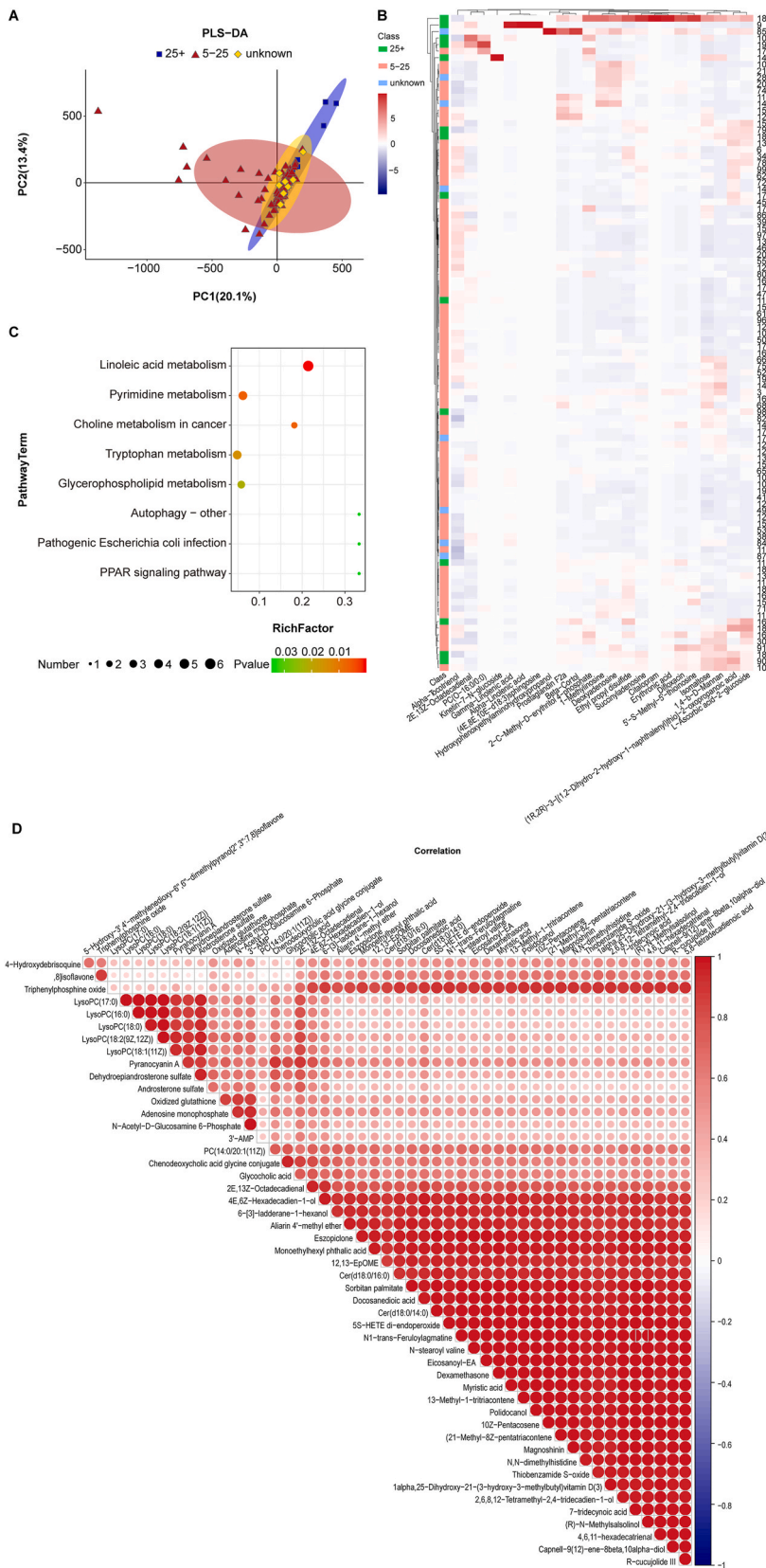
Metabolic dysregulation is a hallmark of different diseases [15], and previous studies have revealed metabolic biomarkers of cervical cancer in plasma [22], feces [23], urine [24], and tumor tissues [25]. Host epithelium, filtrating immune cells, and microbes directly interact with each other in the cervicovaginal microenvironment. However, the metabolome of the cervicovaginal microenvironment of the healthy cervix, cervical neoplasia and cancer have not been comprehensively explored.

Oxidative damage is related to the pathogenesis of cervical cancer, and epidemiological studies have shown that the serum of cervical cancer patients contains high levels of oxidative markers. Aflatoxins are well-known mutagens and carcinogens that are recognized biomarkers of cancer risk in humans. Carvajal et al. found out that the presence of aflatoxin B1 led to a six-fold increase in the risk for cervical cancer [26,27], (OR 6.1, 95 % CI = 1.4–25.4), which is consistent with our study.

We observed high levels of nucleic acid and energy metabolites, such as 3'-UMP, cyclic pyranopterin monophosphate, guanosine monophosphate, 3'-AMP, adenosine monophosphate, and 2'-deoxyguanosine 5'-monophosphate, in the CVL samples of the ICC group compared to N and CIN groups. This could be explained by enhanced DNA synthesis and degeneration caused by increased cell proliferation and necrosis in the tumor microenvironment. Adenosine monophosphate and cyclic pyranopterin monophosphate are effective immune inhibitors [27]. Hence, enrichment of nucleic acids in the cervicovaginal microenvironment might be an emerging hallmark of cancer metabolism [15].

The present study identified communities characterized by enriched microbial genera such as *Gardnerella*, *Prevotella*, *Streptococcus*, and *Atopobium* and by the depletion of *Lactobacillus* [18]. These enriched genera are commonly observed in BV patients [28–31], indicating the important role of microbiota in carcinogenesis. This result points to a way to prevent cervical carcinoma by increasing *Lactobacillus* in the cervicovaginal microenvironment.

We are not aware of any published studies investigating the mechanism underlying the interaction between vaginal bacteria and hosts, except for those reported in clinical studies. Additionally, comprehensive profiling studies of the metabolic processes in the cervicovaginal microenvironment relevant to the microbiome are lacking. Our study was designed to elucidate the metabolomic profiles of cervicovaginal lavage and vaginal microbiota in normal cervix, cervical intraepithelial neoplasia, and carcinoma patients.



(caption on next page)

Fig. 6. Vaginal microbiota was related to an inflammatory microenvironment, which was reflected in metabolites correlated with cervical intra-epithelial neoplasia. A. PLS-DA showing that the high and low status of genital inflammation was significantly different according to the metabolome (MANOVA, Wilk's lambda test, $p = 0.001$); B. Metabolomic heatmap showing two clusters, with grouping based on high and low status of genital inflammation; C. Patients with high status of genital inflammation had higher concentrations of metabolites related to the biosynthesis of unsaturated fatty acids; D-F. Relationship between the high status of genital inflammation and LD microbiota compared to the low status of inflammation and NLD microbiota; G-I. Change trend of alpha-lactose, glycogen, and isomaltose among groups.

The sample size per group in this study was relatively small, which may compromise the statistical power. However, we believe that the inclusion of the consecutive tissues in separate groups renders our results reliable. Another limitation lies in the mass spectroscopy technique itself as some rare metabolites might be missed, which can be addressed in a future study with improved metabolomics coverage.

Collectively, the cervicovaginal metabolome and microbiome demonstrated that metabolic fingerprinting of the cervicovaginal microenvironment could be a reliable discriminator of individuals with cervical dysplasia and ICC. Moreover, our analysis revealed that non-Lactobacillus communities were enriched in cervical carcinoma, and that differential species and metabolites were correlated. In conclusion, the complex host-microbe interplay in the cervicovaginal microenvironment generates unique metabolic fingerprints that could be exploited for diagnosis and therapeutics to ultimately improve women's health.

Funding

This research did not receive any specific grant from funding agencies in the public, commercial, or not-for-profit sectors.

Ethics declarations

The ethics committee of Xiangya Hospital of Central South University approved our study (Approval No.: 202101030) and we obtained written informed consent for participation and publication from each study participant.

Data availability statement

Data relevant to the study have not yet been deposited into a publicly available repository. All data needed to evaluate the conclusions in the paper are present in the paper and the Supplementary Materials. Additional data related to this paper may be requested from the corresponding authors.

CRedit authorship contribution statement

Jie Ou: Writing – original draft, Visualization, Validation, Methodology, Formal analysis, Conceptualization. **Yanan Kang:** Visualization, Formal analysis, Data curation. **Medlegeh:** Writing – original draft, Visualization, Formal analysis, Writing – original draft, Visualization, Formal analysis. **Kun Fu:** Writing – original draft, Visualization, Formal analysis. **Yu Zhang:** Writing – review & editing, Supervision, Project administration, Methodology. **Wenqing Yang:** Writing – review & editing, Supervision, Project administration, Conceptualization.

Declaration of competing interest

The authors declare that they have no known competing financial interests or personal relationships that could have appeared to influence the work reported in this paper.

Acknowledgments

Authors express their gratitude and appreciation to all persons who contributed in this manuscript.

Appendix A. Supplementary data

Supplementary data to this article can be found online at <https://doi.org/10.1016/j.heliyon.2024.e33383>.

References

- [1] F. Bray, J. Ferlay, I. Soerjomataram, R.L. Siegel, L.A. Torre, A. Jemal, Global cancer statistics 2018: GLOBOCAN estimates of incidence and mortality worldwide for 36 cancers in 185 countries, *CA Cancer J Clin* 68 (2018) 394–424, <https://doi.org/10.3322/caac.21492>.
- [2] M. Schiffman, N. Wentzensen, S. Wacholder, W. Kinney, J.C. Gage, P.E. Castle, Human papillomavirus testing in the prevention of cervical cancer, *J Natl Cancer Inst* 103 (2011) 368–383, <https://doi.org/10.1093/jnci/djq562>.

- [3] A. Mitra, D.A. MacIntyre, J.R. Marchesi, Y.S. Lee, P.R. Bennett, M. Kyrgiou, The vaginal microbiota, human papillomavirus infection and cervical intraepithelial neoplasia: what do we know and where are we going next? *Microbiome* 4 (58) (2016) <https://doi.org/10.1186/s40168-016-0203-0>.
- [4] S.M. Gupta, J. Mania-Pramanik, Molecular mechanisms in progression of HPV-associated cervical carcinogenesis, *J. Biomed. Sci.* 26 (28) (2019), <https://doi.org/10.1186/s12929-019-0520-2>.
- [5] M. Wahid, S.A. Dar, A. Jawed, R.K. Mandal, N. Akhter, S. Khan, F. Khan, S. Jogaiah, A.K. Rai, R. Rattan, Microbes in gynecologic cancers: causes or consequences and therapeutic potential, *Semin. Cancer Biol.* 86 (2021) 1179–1189, <https://doi.org/10.1016/j.semcancer.2021.07.013>.
- [6] E. Gillet, J.F. Meys, H. Verstraelen, C. Bosire, P. De Sutter, M. Temmerman, D.V. Broeck, Bacterial vaginosis is associated with uterine cervical human papillomavirus infection: a meta-analysis, *BMC Infect. Dis.* 11 (10) (2011), <https://doi.org/10.1186/1471-2334-11-10>.
- [7] Y.L. Guo, K. You, J. Qiao, Y.M. Zhao, L. Geng, Bacterial vaginosis is conducive to the persistence of HPV infection, *Int. J. STD AIDS* 23 (2012) 581–584, <https://doi.org/10.1258/ijisa.2012.011342>.
- [8] A. Mitra, D.A. MacIntyre, Y.S. Lee, A. Smith, J.R. Marchesi, B. Lehne, R. Bhatia, D. Lyons, E. Paraskevidis, J.V. Li, E. Holmes, J.K. Nicholson, P.R. Bennett, M. Kyrgiou, Cervical intraepithelial neoplasia disease progression is associated with increased vaginal microbiome diversity, *Sci. Rep.* 5 (16865) (2015), <https://doi.org/10.1038/srep16865>.
- [9] A. Audirac-Chalifour, K. Torres-Poveda, M. Bahena-Roman, J. Tellez-Sosa, J. Martineze-Barnette, B. Cortina-Ceballos, G. Lopez-Estrada, K. Delgado-Romero, A. I. Burguete-Garcia, D. Cantu, A. Garcia-Carranca, V. Madrid-Marina, Cervical microbiome and cytokine profile at various stages of cervical cancer: a pilot study, *PLoS One* 11 (e0153274) (2016), <https://doi.org/10.1371/journal.pone.0153274>.
- [10] A. Mitra, D.A. MacIntyre, G. Ntrisos, A. Smith, K.K. Tsilidis, J.R. Marchesi, P.R. Bennett, A.B. Moscicki, M. Kyrgiou, The vaginal microbiota associates with the regression of untreated cervical intraepithelial neoplasia 2 lesions, *Nat. Commun.* (2020) 11, <https://doi.org/10.1038/s41467-020-15856-y>, 1999.
- [11] J. Norenhag, J. Du, M. Olovsson, H. Verstraelen, L. Engstrand, N. Brusselaers, The vaginal microbiota, human papillomavirus and cervical dysplasia: a systematic review and network meta-analysis, *BJOG* 127 (2020) 171–180, <https://doi.org/10.1111/1471-0528.15854>.
- [12] C. Violán, A. Roso-Llorach, Q. Foguet-Boreu, M. Guisado-Clavero, M. Pons-Vigués, E. Pujol-Ribera, J.M. Valderas, Multimorbidity patterns with K-means nonhierarchical cluster analysis, *BMC Fam. Pract.* 19 (108) (2018), <https://doi.org/10.1186/s12875-018-0790-x>.
- [13] E. Motevaseli, M. Shirzad, S.M. Akrami, A.S. Mousavi, A. Mirsalehian, M.H. Modarresi, Normal and tumour cervical cells respond differently to vaginal lactobacilli, independent of pH and lactate, *J. Med. Microbiol.* 62 (2013) 1065–1072, <https://doi.org/10.1099/jmm.0.057521-0>.
- [14] D.S. Wishart, R. Mandal, A. Stanislaus, M. Ramirez-Gaona, Cancer metabolomics and the human metabolome database, *Metabolites* (2016) 6, <https://doi.org/10.3390/metabo6010010>.
- [15] N.N. Pavlova, C.B. Thompson, The emerging hallmarks of cancer metabolism, *Cell Metab* 23 (27–47) (2016), <https://doi.org/10.1016/j.cmet.2015.12.006>.
- [16] Y. Zhu, G. Sun, Y. Cidan, B. Shi, Z. Tan, F. Sun, L. Ning, H. Han, J. Wang, W. Basang, Multi-omics Analysis to Examine Microbiota and Metabolites in the Colon of Different Breeds of Swine, 2022.
- [17] X. Jian, Y. Zhu, J. Ouyang, Y. Wang, Q. Lei, J. Xia, Y. Guan, J. Zhang, J. Guo, Y. He, J. Wang, J. Li, J. Lin, M. Su, G. Li, M. Wu, L. Qiu, J. Xiang, L. Xie, W. Jia, W. Zhou, Alterations of gut microbiome accelerate multiple myeloma progression by increasing the relative abundances of nitrogen-recycling bacteria, *Microbiome* 8 (74) (2020), <https://doi.org/10.1186/s40168-020-00854-5>.
- [18] Z.E. Ilhan, P. Łaniewski, N. Thomas, D.J. Roe, D.M. Chase, M.M. Herbst-Kralovetz, Deciphering the complex interplay between microbiota, HPV, inflammation and cancer through cervicovaginal metabolic profiling, *EBioMedicine* 44 (2019) 675–690, <https://doi.org/10.1016/j.ebiom.2019.04.028>.
- [19] P. Łaniewski, D. Barnes, A. Goulder, H. Cui, D.J. Roe, D.M. Chase, M.M. Herbst-Kralovetz, Linking cervicovaginal immune signatures, HPV and microbiota composition in cervical carcinogenesis in non-Hispanic and Hispanic women, *Sci. Rep.* 8 (7593) (2018), <https://doi.org/10.1038/s41598-018-25879-7>.
- [20] R.B. Ness, K.E. Kip, S.L. Hillier, D.E. Soper, C.A. Stamm, R.L. Sweet, P. Rice, H.E. Richter, A cluster analysis of bacterial vaginosis-associated microflora and pelvic inflammatory disease, *Am. J. Epidemiol.* 162 (2005) 585–590, <https://doi.org/10.1093/aje/kwi243>.
- [21] N. Brusselaers, S. Shrestha, J. van de Wijgert, H. Verstraelen, Vaginal dysbiosis and the risk of human papillomavirus and cervical cancer: systematic review and meta-analysis, *Am. J. Obstet. Gynecol.* 221 (9–18.e18) (2019), <https://doi.org/10.1016/j.ajog.2018.12.011>.
- [22] K. Yang, B. Xia, W. Wang, J. Cheng, M. Yin, H. Xie, J. Li, L. Ma, C. Yang, A. Li, X. Fan, H.S. Dhillon, Y. Hou, G. Lou, K. Li, A comprehensive analysis of metabolomics and transcriptomics in cervical cancer, *Sci. Rep.* 7 (43353) (2017), <https://doi.org/10.1038/srep43353>.
- [23] Y. Chai, J. Wang, T. Wang, Y. Yang, J. Su, F. Shi, J. Wang, X. Zhou, B. He, H. Ma, Z. Liu, Application of 1H NMR spectroscopy-based metabolomics to feces of cervical cancer patients with radiation-induced acute intestinal symptoms, *Radiother. Oncol.* 117 (2015) 294–301, <https://doi.org/10.1016/j.radonc.2015.07.037>.
- [24] N. Ye, C. Liu, P. Shi, Metabolomics analysis of cervical cancer, cervical intraepithelial neoplasia and chronic cervicitis by 1H NMR spectroscopy, *Eur. J. Gynaecol. Oncol.* 36 (2015) 174–180.
- [25] B. Sitter, T. Bathen, B. Hagen, C. Arentz, F.E. Skjeldestad, I.S. Gribbestad, Cervical cancer tissue characterized by high-resolution magic angle spinning MR spectroscopy, *Magma* 16 (2004) 174–181, <https://doi.org/10.1007/s10334-003-0025-5>.
- [26] C.R. Santos, A. Schulze, Lipid metabolism in cancer, *FEBS J.* 279 (2012) 2610–2623, <https://doi.org/10.1111/j.1742-4658.2012.08644.x>.
- [27] I. Perrot, H.A. Michaud, M. Giraudon-Paoli, S. Augier, A. Docquier, L. Gros, R. Courtois, C. Dejoui, D. Jecko, O. Becquart, H. Rispaud-Blanc, L. Gauthier, B. Rossi, S. Chanteux, N. Gourdin, B. Amigues, A. Roussel, A. Bensussan, J.F. Eliaou, J. Bastid, F. Romagne, Y. Morel, E. Narni-Mancinelli, E. Vivier, C. Patureau, N. Bonnefoy, Blocking antibodies targeting the CD39/CD73 immunosuppressive pathway unleash immune responses in combination cancer therapies, *Cell Rep.* 27 (2019) 2411–2425 e2419, <https://doi.org/10.1016/j.celrep.2019.04.091>.
- [28] P. Shannon, A. Markiel, O. Ozier, N.S. Baliga, J.T. Wang, D. Ramage, N. Amin, B. Schwikowski, T. Ideker Cytoscape, A software environment for integrated models of biomolecular interaction networks, *Genome Res.* 13 (2003) 2498–2504, <https://doi.org/10.1101/gr.1239303>.
- [29] J.G. Caporaso, J. Kuczynski, J. Stombaugh, K. Bittinger, F.D. Bushman, E.K. Costello, N. Fierer, A.G. Pena, J.K. Goodrich, J.I. Gordon, G.A. Huttley, S.T. Kelley, D. Knights, J.E. Koenig, R.E. Ley, C.A. Lozupone, D. McDonald, B.D. Muegge, M. Pirrung, J. Reeder, J.R. Sevinsky, P.J. Turnbaugh, W.A. Walters, J. Widmann, T. Yatsunenko, J. Zaneveld, R. Knight, QIIME allows analysis of high-throughput community sequencing data, *Nat. Methods* 7 (2010) 335–336, <https://doi.org/10.1038/nmeth.f.303>.
- [30] H. Wickham, ggplot2: elegant graphics for data analysis, Springer International Publishing : Imprint: Springer (2016), <https://doi.org/10.1007/978-3-319-24277-4> (1 online resource (XVI, 260 pages 232 illustrations, 140 illustrations in color).
- [31] B. Goodman, H. Gardner, The microbiome and cancer, *J. Pathol.* 244 (2018) 667–676, <https://doi.org/10.1002/path.5047>.